Fabrication and testing of crop waste Ceiba Pentandra Shell Powder reinforced biodegradable composite films

Kaliraj M
AAA College of Engineering and Technology
Narayanasamy P (narayananx5@gmail.com)
Kamaraj College of Engineering and Technology https://orcid.org/0000-0002-1436-8338
Balavairavan B
Kamaraj College of Engineering and Technology https://orcid.org/0000-0002-7646-2792
Balasundar P
Kamaraj College of Engineering and Technology https://orcid.org/0000-0002-3578-3733

Research Article

Keywords: Crop residues, Ceiba Pentandra Shell, biodegradable packaging films

Posted Date: August 14th, 2023

DOI: https://doi.org/10.21203/rs.3.rs-3159403/v1

Abstract

Ceiba Pentandra Shell Powder (CPSP) bio waste is chosen as a bio filler combined with Polyvinyl Alcohol (PVA) as a matrix to make biofilms to increase the exploitation of bio waste materials and reduce the use of plastic materials. The fabricated biofilms endured the structural, thermal, microstructural, mechanical, UV barrier, opacity, water absorption, and soil burial properties. FTIR plots indicated no significant chemical reaction or formation of new functional groups during an interaction between PVA and CPSP. XRD diffractograms represented the crystallinity index (35.3, 38.6, 42.3, 46.4 and 48.5%) and crystalline size (18.14, 20.89, 23.23, 24.87and 26.34 nm) of biofilms increased with CPSP loading (5–25 wt. %). The PVA/CPSP films are thermally stable up to 322 °C. The peak highs of AFM images showed that the films surface roughness gradually increased from 94.75 nm (5 wt. % CPSP) to 320.17 nm (25 wt. % CPSP). The FESEM micrographs clarify the homogenous distribution of CPSP materials in the PVA matrix. Tensile strength and tensile modulus are noticeably increased by 26.32% and 37.92%, respectively, due to the loading of CPSP from 5 wt. % to 20 wt. % in the PVA matrix. The PVA/CPSP films outperform than pure PVA films in UV shielding (350–450 nm). The 59% of weight loss of films was estimated during 60 days of burial time. Overall, PVA/ CPSP (5–25 wt. %) films are biodegradable and have promising applications as good packaging material.

Introduction

Plastics are now becoming a core component for many applications such as automobile, packaging, furniture’s and house old appliances etc. Since we produced and discarded so many plastics, our necessity for plastic has another graver drawback [1]. In the 9 billion tonnes of plastic produced around the world as 2010, 6.9 billion tonnes have been wasted and just 9% have been recycled. The remaining plastic garbage is disposed of in landfills and waterways around the globe, where it causes pollution that harms the species [2, 3]. Ineffective packaging plastics comprise about 40% of the garbage. The development of environmentally friendly products has received a lot of attention recently, with ecofriendly materials being used as a probable replacement in lieu of plastic (derived from petroleum hydrocarbons) packaging materials [4]. The various benefits of bio-composite materials include their relative affordability, increased environmental friendliness, and inherent biodegradability [5].

The production of bio films with synthetic polymers as an alternative to packaging plastics that can provide high mechanical properties and non-venomous will be suitable for food packaging, biomedical, and enclosing applications [6, 7]. In various fields, polyvinyl alcohol (PVA) is overtaking other non-biological polymers like polyethylene, polypropylene, HDPE, etc. because it has the properties of biodegradability, non-toxicity, hydrophilic, film forming and higher tensile strength [8, 9]. Specifically, PVA is acknowledged as one of the most promising biodegradable polymers in mulch films [10]. PVA has some downsides, including a high degree of hydrophilicity due to PVA originating with more hydroxyl groups in its carbon chains and a sluggish decomposition rate in anaerobic environment [11]. To improve the mechanical properties, biodegradation rate, and hydrophilic nature of PVA-based composites, combining them with organic fillers extracted from plant wastes may be viable [12]. The crop scums, farming rubbishes, and by-products are suitable biological reinforcement fillers for bio-composites [13]. Combining plant leftovers with polymeric materials results in a composite material with enhanced properties.

The Malvaceae tree family includes the genus Ceiba, indigenous to tropical and subtropical regions of the Americas and tropical West Africa. The Ceiba Pentandra (Kapok) plant yields a strong and lightweight fiber used to stuff dolls, pillows, mattresses, and tapestries [14]. The most prominent textile fiber is lint, produced from cotton, the king of natural fiber, collected from the torn Ceiba Pentandra fruits [15]. Lint is the most comfortable and environmentally friendly textile fiber. Oils used to prepare fertilizers and soap are extracted from the seeds of the Ceiba tree [16]. Due to their high fiber and tannin content, Ceiba Pentandra seeds reportedly had a low feeding value. The bulk of the stalk is burnt off in the fields after the cotton crop harvest. The outer Shells of ripped Ceiba Pentandra fruits are leathery, pendulous capsules 10–25 cm long and 3–6 cm in diameter [17]. The mature fruit shells of Ceiba Pentandra are underused and are more fibrous and biodegradable [18]. A thorough analysis of the scientific literature indicated that the ripped fruit shell powder from Ceiba Pentandra has not yet been documented as a reinforcement filler for PVA-based biofilms. In the framework, the objective of this work is to explore the effects of Ceiba Pentandra Shell Powder content (5, 10, 15, 20, and 25 **wt.%**) in PVA matrix on structural, mechanical, thermal, water resistance, UV-barrier, optical, biodegradable and antimicrobial properties of the resultant bio composite films. The information gained from this study will provide an excellent foundation for the practical uses of Ceiba Pentandra ripped fruit shell powder, which may be appropriate for bio-based packaging and enfolding materials.

Materials

Poly (vinyl alcohol), PVA, 97% hydrolyzed, (molecular weight of 1,20,000 and 1% ash max) and deionized water was got from Nice chemicals (P) LTD, Kochi, Kerala, India. PVA granules were white and were kept in a sealed container. The ripped fruit shells were collected from a local cotton farm in Rajapalayam, Tamilnadu, India. The cotton inside ripped fruits of kapok is removed, and the outer shells are dried and crushed into nano-sized reinforcement filler. The average particle size of the Ceiba Pentandra Shell powder was 130.34 nm measured by using Micro trap optical particle size analyzers.

Fabrication of PVA/CPSP biofilms

The preparation of Ceiba Pentandra Shell powder and PVA/CPSP biofilms shown in Fig. 1. The PVA/CPSP biofilms were made-up via solution casting method. 20 ml of deionized water was measured and poured into a beaker containing 2 g of hot water soluble polyvinyl alcohol (PVA). Nearly two hours of continuous magnetic stirring at 90 °C were employed to prepare the homogeneous PVA solution. The different proportions (5, 10, 15, 20 and 25wt.%) of CPSP was mixed with PVA solution and stirred for 2 hours to get a consistent PVA/CPSP polymer solution. The mixture was then poured over the Petri dishes and allowed to dry for 12 hours at room temperature. After that, films were de-moisturized for two hours at 50°C in the oven. For each combination of PVA and powdered Ceiba Pentandra shell, five film samples were generated. The film, with an average thickness of 0.141 mm, was peeled off and desiccated for further characterization.

Experimental Methods

Fourier-transform infrared spectroscopy Analysis (FTIR)

The functional group of samples (PVA matrix, Ceiba Pentandra Shell Powder, and the PVA/CPSP bio composite films) was analysed using Fourier transform infrared spectroscopy (RXI Perkin Elmer). The film samples were reshaped into 10 mm × 10 mm for testing. The sample was placed on the base optics assembly, and the spectra were recorded. The characterization ranged from 4000 to 500 cm-1 in 45 times scanning to reduce noise and prevent spectrum overlapping at a resolution of 4 cm^{-1}.

X-ray Diffraction (XRD)

An X-ray powder Diffractometer analysed the crystallinity and crystalline size of PVA, Ceiba Pentandra Shell Powder and fabricated PVA/CPSP biofilms. The intensity in the 2θ range from 6° to 40° at 4° /min obtained in the XRD (XPERT-PRO) was used to calculate the Crystallinity index (CI) according to Equation [19].

$$\mathrm{CI} = \left[\frac{\mathrm{I}_{200} - \mathrm{I}_{100}}{\mathrm{I}_{200}} \times 100\right] \quad (1)$$

Where I_{200} indicates the crystalline phase (2θ = 21–34°) and I_{100} indicates the amorphous phase (2θ = 17–20°)

The crystalline size of samples calculated, according to Scherer's Equation [20],

$$\text{Crystallite size} = \left[\frac{\mathrm{k}\lambda}{\beta.\cos\theta}\right] \quad (2)$$

Where K = Scherrer's constant (0.89), λ = wavelength of the radiation (0.1541 nm), β = FWHM (Full Width Half Maximum)

Atomic Force Microscopy (AFM)

The surface roughness and structure observation of PVA/CPSP films carried out by AFM model: Park XE-70. The PVA/CPSP film samples were resized to 45 mm x 45 mm to measure their surface roughness. The test was conducted in a closed loop with a large area scanner XY > 90μm, Z > 7.5 μm, and XY noise < 1.2 nm RMS, typical imaging bandwidth. For PVA/CSPS film samples, the surface roughness parameters Ra, Rq, Rsk, and Rku were evaluated. Ra stands for average roughness, Rq for root mean square roughness, Rsk for skewness, and Rku for kurtosis.

TGA &DTG

Thermogravimetry Analysis (TGA) and differential thermogravimetry (DTG) of PVA, Ceiba Pentandra Shell Powder, and PVA/CPSP biofilms were executed by using thermo gravimetric analyser (TGA, NETZSCH STA 449F3-1100-M). Samples of about 2.5 mg kept in an alumina chamber were heated at 50–550℃ at a heating range of 10℃/min under a nitrogen atmosphere.

Tensile testing

Tensile strength, Tensile modulus, and % elongation at break of the pure PVA and PVA/ CPSP (5–25 wt. %) biofilms were measured by a Universal Testing Machine (INSRON 3369 – ASTM D3039) [21]. Five samples in each proportion with 100 mm x 10 mm were used. The machine specifications are machine speed: 100 mm/min, gauze length: 8 cm, and load: 500 N, respectively.

FESEM

The FESEM images of PVA, CPSP, and PVA/CPSP biofilms were obtained on a Field Emission scanning electron microscope (FESEM -SIGMA HV–Carl Zeiss). The experimental constraints were a resolution of 1000x magnification and an acceleration voltage of 20 kV. All film samples were cut into small pieces, which were then sputtered with gold to turn the film samples into conductive.

Ultraviolet- visible (UV-vis) Spectrograph

The transmittance of pure PVA and PVA/ CPSP (5–25 wt.%) biofilms were measured using an ultraviolet-visible spectrophotometer (Model 8451A, Hewlett–Packard Co., and Santa Clara, CA, USA). The film samples were (30 mm x 30 mm) square shape and measured in the series of wavelengths from 200 to 800 nm at a scanning rate of 200 nm/minute.

The following Equation calculated the opacity of the films [22].

Opacity = $\left[\mathrm{absorbanceat600nm} \times \mathrm{filmthickness}\right]$ (3)

Water Intake

The % of water inhaling of the pure PVA and PVA/CPSP (5–25 wt. %) biofilms was measured according to ASTM D570 [23]. The 50 mm x 50 mm cross-section of films were de-moisturized in a vacuum oven at 50°C for 24 hours, then chilled in a desiccator, and then promptly weighed (w_{dry}). The films were then completely soaked in distilled water at ambient temperature for the equilibrium test (24 h). The water on the film surface was detached after removing it from the container using filter paper. Afterward, each film was weighed (w_{wet}). The % of water intake of PVA/CPSP biofilm is calculated by using the following Equation.

Water intake (%) = $\left[\frac{\mathrm{w}_{\mathrm{dry}}-\mathrm{w}_{\mathrm{wet}}}{\mathrm{w}_{\mathrm{dey}}} \times 100\right]$ (4)

Soil burial test

The indoor soil burial test explored the biodegradability of pure PVA and PVA/CPSP (5–25 wt. %) biofilms using the methodology of Balavairavan et al. 2012 [24]. Initially, the vacuum-dried sample weighed 0.62 g (Wi). Further, the film samples which had been vacuum-dried were buried separately in mud pots containing moist soil. The mud pots carrying the film samples (PVA and PVA/CPSP) were brooded at 23°C for two months. Water was sprayed on the mud pots regularly to keep them damp. The film samples were taken from the mud pots once in ten days to estimate the weight loss. The film samples were meticulously cleaned with water to remove the dust and then dried under Hoover until the constant weight (W_T) was achieved. The total % weight loss of film samples was calculated using the following Equation.

% Wt. Loss of film $= \left[\frac{\text{Initialwt.atthebeginning} - \text{Finalwt.after10days}}{\text{Initialwt.atthebeginning}} \times 100\right]$ (5)

Result and Deliberation

Fourier Transform Interferometry (FTIR)

The spectra of PVA (Fig. 2 **(a)**) showed a broader peak at 3290.36 cm^{-1} owing to the stretching vibration of the hydroxyl group. The ranges of PVA showed a C-H stretching of aldehyde at 2792.72 cm^{-1} and 2724.14 cm^{-1}. The stretching band found at 1625.78 cm^{-1} shows the C = C group of alkenes. The peak at 1521.63 cm^{-1} is due to C-O carbonyl stretching, the peak at 1133.93 cm^{-1} and account of C-H bending vibration of CH_2, peak at 1133.93^{-1} is due to C-H deformation vibration [25].

The FTIR spectra of (Fig. 2 **(a)** ceiba pentandra shell powder showed the presence of –OH stretching (3400–3650 cm^{-1}), –CH stretching (2148.48 cm^{-1}), the intermolecular hydrogen bonding (1629.63 cm^{-1}), C = C stretching of cyclic alkene (819.56 cm^{-1}, 906.33 cm^{-1} and 1546.69 cm^{-1}) respectively. As shown in Fig. 2**(b)**, with increasing the Ceiba Pentandra Shell Powder, the peak at 3290.36 cm^{-1} (PVA) shifted to a higher wavenumber in the region of 3330 to 3560 cm^{-1} for all proportions of films. The lengthy flat peak of –OH bonds assimilated in all combinations films is similar to the peaks of CPSP. This may be because CPSP and PVA formed robust hydrogen bonds with one another. The characteristic peak of C-H vibration from cellulose and hemicellulose was noticed in the infrared spectra at 2991.59 cm^{-1} (This peak sifted to higher numbers in case films). The peaks at 1652.99 cm^{-1} and 1564.33 cm^{-1} reflected the aromatic C = C band, which merely occurs in lignin, showing that the lignin has been preserved in the shell particles of Ceiba pentandra. The 1178.50 cm^{-1} represented the bending of C-O stretching, a common peak for films containing CPSP up to 20 wt. %. The peak at 1178.50 cm^{-1} vanished at maximum filler material loading (25 wt. %), and smooth IR spectra were seen. In PVA/CPSP films, the posse at 875.68 cm^{-1} is visible due to the C = C bending of alkane up to 20 wt. % of filler; however, this peak also extinct further CPSP loading. Overall, the good compatibility between PVA and CPSP is due to strong –OH bonding. Notably, in contrast to the peak patterns of PVA and CPSP, neither a significant band displacement nor a new peak pattern emerged in the PVA/CPSP biofilm. This might result from the little chemical interaction between the constituent parts.

X-Ray Diffraction (XRD)

X-ray diffraction test provides the valuable data related to base materials and films samples degree of crystallinity and crystalline size. The X-ray outlines of PVA, CPSP, and PVA/CPSP films containing CPSP are shown in Fig. 3 **(a & b)**. X-ray diffraction patterns of the PVA displayed the scattering peak in the region from 2θ = 10° to 47.2° by the counts at 2θ = 19.17°. The Ceiba Pentandra Shell Powder shows sharp peaks at 2θ = 19.95°, 29.88°, 32.60° and 48.04°, demonstrating that CPSP is I crystalline.

The PVA/CPSP film containing 5, 10, 15, 20, and 25% CPSP showed the peaks with the counts at 2θ = 19.40°, 2θ = 19.83°, 2θ = 19.93°, 2θ = 20.01° and 2θ = 19.81° respectively. The XRD patterns of PVA/CPSP films exposed that all the film samples are partly crystalline with a distinctive peak at 2θ = 20°. According to B. Aziz et al. (2020) [26] and Mori et al. (2020) [27], the XRD peak of PVA showed the wide signal characteristic for amorphous phase occurs at about 2θ = 19°. The XRD pattern of Ceiba Pentandra Shell Powder indicated the high crystalline peak at 2θ = 19.95°. The crystallinity Index and crystalline size of PVA, CPSP, and PVA/CPSP biofilms are shown in Table 1. The crystallinity index of pure PVA is least value comparing to all the film combinations. With the addition of CPSP filler (5–25 wt.%) the crystallinity index of PVA/CPSP biofilms accelerated up to 27.12% the increase in crystallinity index indicates the physical structure of biofilm enhanced and also appropriate stress transfer occurred between matrix to filler orientations. The increase of crystalline size corresponding to addition of CPSP in PVA matrix exhibited that the surface roughness of biofilms increased and resistance to withstand deformation under external load also enriched.

Table 1
Crystallinity Index and Crystalline size of PVA, CPSP and PVA/CPSP biofilms

Samples	Crystallinity Index (%)	Crystalline size (nm)	Physical nature
Pure PVA	33.2%	17.34	Amorphous
Ceiba Pentandra Shell Powder	53.5%	32.34	Crystalline
PVA/5wt.% CPSP	35.3%	18.14	Semi crystalline
PVA/10wt.% CPSP	38.6%	20.89	Semi crystalline
PVA/15wt.% CPSP	42.3%	23.23	Semi crystalline
PVA/20wt.% CPSP	46.4%	24.87	Semi crystalline
PVA/25wt.% CPSP	48.5%	26.34	Semi crystalline

Atomic Force Microscopy (AFM)

Atomic Force Microscopy can quantify the surface coarseness of samples down to the angstrom-scale (0.1 nm). [28] In order to evaluate the topological features of the produced PVA/CPSP films, atomic force microscopy (AFM) was used. Phase contrast, histograms, roughness parameter, and 2D and 3D pictures were recorded. As seen in Fig. 4(a-e), the films exhibited both a smooth surface and some surface agglomerations at increasing wt. % of CPSP, with a Root Mean Square roughness (RMS) of a few nm. The agglomerated designs resemble separate peaks, each measuring 1 µm in width and 80–260 nm in height. Particles in these structures range in size from 10 to 50 nm. The value of the phase contrast for all samples is about 5°–10°, indicating good homogeneity and no phase separations up to 20% of CPSP in PVA matrix. AFM parameters of PVA/CPSP (5–25 wt. %) biofilms are listed in Table 2.

Table 2
AFM parameters of PVA/CPSP (5-25wt.) biofilms

Film sample	**Min (nm)**	**Max (nm)**	**Mid (nm)**	**Mean (nm)**	**Rpv (nm)**	**Rq (nm)**	**Ra (nm)**	**RMS (nm)**	**Rsk**	**Rku**
PVA /5 wt.% CPSP	-25.75	68.99	21.61	0.00	94.75	16.98	11.04	83.75	-2.352	8.25
PVA /10 wt.% CPSP	-29.08	78.46	24.68	0.00	107.55	18.37	12.11	93.71	-2.067	8.67
PVA /15 wt.% CPSP	-61.23	138.14	38.45	0.00	199.38	29.48	30.62	141.8	-1.118	4.08
PVA /20 wt.% CPSP	-76.59	161.06	42.23	0.00	237.65	38.94	21.02	161.4	-1.113	6.53
PVA /25wt.% CPSP	-86.82	233.35	73.26	0.00	320.17	72.50	52.91	252.5	-1.891	5.46

A low surface roughness, at about 20–25 nm, can be observed in the PVA film. Adding CPSP evidenced increased RMS to 82–84 nm, 91–95 nm, 138–142 nm, 157–163 nm, and 250–253 nm with increased CPSP content 5, 10, 15, 20 and 25wt.% respectively in the PVA matrix. This might be caused by CPSP's partial water insolubility; however, it can change the surface roughness while high concentrations in the PVA matrix.

TGA and DTG

To analyze the thermal stability and decomposition properties of films containing various concentrations (5–25 wt. %) of Ceiba Pentandra Shell Powder in a PVA matrix, thermo-gravimetric analysis was performed. TGA is a significant analysis used to examine bio film's thermal behaviour and degradation. Figure 5 **(a&b) s**howed the thermogravimetric (TGA) and derivative thermogravimetric (DTG) curves of PVA, Ceiba Pentandra Shell Powder, and PVA/CPSP (5–25 wt. %) film samples. All curves followed a similar pattern, demonstrating that the PVA-based films thermal degradation and mass loss ensued in three unique stages, each accompanied by a peak in the DTG curve that correlated to a distinct heating region. The initial thermal response induced the initial mass loss, which occurred below 100°C. This was primarily because moisture and water vapour were eliminated [29]. Accordingly, PVA and PVA/CPSP films showed the considerable weight loss compared to Ceiba Pentandra Shell Powder. This observation is most likely explained by the high moisture content found across every combination of test samples. Thus, presence of higher moisture content the higher the mass loss arisen in this phase. The second weight loss happened at temperatures between 150°C and 290°C after additional heating. The degradation of polymeric chains (cellulose, hemicellulose) and water residues was primarily responsible for this mass loss. Similar findings were previously reported by [30]. The film sample final mass loss occurred at temperatures greater than 270°C. The depolymerization and breakdown of the carbon chains in the PVA structure was responsible for the weight loss during this stage. From the data in Table 3, all films exhibited close decomposition temperatures that varied between 290 and 322^{o}C, higher than the controlled PVA's degradation temperature, which recorded its maximum decomposition at 288∘C and less than the CPSP which recorded its decomposition temperature at 341∘C. This evidence that the incorporation of Ceiba Pentandra Shell Powder enhanced the thermal stability of PVA/CPSP biofilm. Such results are consistent with the data obtained in Loganathan and saravanakumar 2022, who also studied the effect of orange peel powder on polyvinyl alcohol films and declared that the rate of degradation of films ranged from 290.9℃ to 295.4℃.

Moreover, the thermal degradation of films was radically influenced by the addition of CPSP at various concentrations (5–25 wt.%), representing the percentage of residue left remained after the final degradation, as shown in Table 4. Adding (5, 10, 15, 20, and 25 wt. %) CPSP in PVA, the % residue increased by 9.23, 10.45, 12.43, 13.98, and 15.49%, respectively. This phenomenon demonstrated that, at temperatures above 320°C, films with high concentrations of CPSP are more heat resistant than PVA films. These annotations aligned with previous studies by researchers investigating the effect of various cassava starch on PVA-based films and indicated that PVA/cassava starch films achieved the thermal stability up to 300℃ [31].

Table 3
Maximum degradation temperature and % residue for PVA, CPSP and PVA/CPSP biofilms

Samples	Degradation Temperature (°C)	% Residue at 545.75°C
PVA	288.78	-1.03
Ceiba Pentandra Shell Powder	341.01	30.05
PVA/5wt.% CPSP	308.04	9.57
PVA/10wt.% CPSP	309.22	9.61
PVA/15wt.% CPSP	312.39	13.07
PVA/20wt.% CPSP	317.61	15.23
PVA/25wt.% CPSP	322.61	15.49

FESEM

FESEM micrographs of PVA, Ceiba Pentandra Shell Powder, and PVA/CPSP biofilms are shown in Fig. 6. FESEM plots **(**Fig. 6 **(a&b))** of PVA and CPSP exhibited smooth and rough surfaces, respectively. The incorporation of CPSP increased the coarser texture of PVA films, which is also confirmed by AFM analysis. The loading of CPSP up to 20 wt. % in the PVA matrix showed a smooth surface with no surface agglomerations. The cross-section of PVA films thickened after CPSP was added, as shown in Fig. 6 **(c–f)**, although all combinations of CPSP (5, 10, 15, and 20 wt.%) in the film matrix seemed to be highly compatible. These results suggested that loading of CPSP up to 20 wt. % are well assimilated in the PVA film. Some agglomeration particles resulting from the inexorable phase separation were evident on the film surface. The agglomeration and voids were observed at 25 wt. % of CPSP may affect the tensile test parameters of PVA-based films. Without significantly compromising the film homogeneity, blocking visible and UV light will be possible by incorporating the Ceiba Pentandra Shell Powder in PVA films.

Mechanical properties

In particular, this study evaluates the tensile stress, Young's modulus, and % of elongation at break for pure PVA films and PVA/CPSP biofilms (5–25 wt. %). Figure 7 shows that the tested films tensile strength increased when CPSP concentration raised from 5 to 20 wt. %. If the filler loading increased beyond the 20 wt. % the transition stage initiated, and the elongation of films increased due to poor compatibility between matrix and filler. This result is consistent with a prior investigation made by [32]. The PVA-based film with 20 wt. % of CPSP documented the highest tensile stress (29.93 MPa), higher than that of films with 25 wt. % CSPS (26.95 MPa) in PVA matrix. The hydrogen bonds that formed between the molecules of PVA and CPSP are thought to be the cause of the high tensile stress at 20 wt. % of CPSP content [33]. These bonds are primarily governed up to 20 weight percent of CPSP and weaken when the concentration increases above 20 wt. %. The maximum tensile strength (29.93 MPa) for PVA/ 20 wt. % CPSP films in the current study were higher than PVA-based films with a mixing of 20 wt. % of nano rice hull fillers observed by 16.86 MPa. Similarly, PVA with 20 wt. % of palm kernel shell powder obtained by 11 MPa is lower than the current study findings.

In essence, the stiffness of materials can be expressed by its Young's modulus (also known as its elastic modulus). It simply refers to how easily it can be stretched or bent. Figure 7 shows that the effect of incorporation of Ceiba Pentandra Shell Powder content (5 – 25 wt. %) on Young's modulus of PVA/CSPS films has the same manner compared with their corresponding tensile stress. The Young's modulus of PVA/CSPS films increased from 21.34 MPa to 65.43 MPa for pure PVA film and PVA/20 wt. % CPSP film respectively. The stiffness of the films faintly diminished from 65.43 MPa to 61.08 MPa as the concentration of Ceiba Pentandra Shell Powder increased from 20 wt.% to 25 wt.%. The better dispersion of CPSP up to 20 wt. % improves their interaction with PVA matrices, thus leading to the higher tensile strength and Young's modulus of PVA/CPSP biofilms. CPSP agglomeration appears to negatively impact tensile strength and Young's modulus, as evidenced by the higher surface roughness and lower tensile strengths of biofilms produced when the amount of CPSP is increased beyond 20 wt.%. [34] Thus, Young's modulus of 25 wt. % of CPSP-loaded films is reduced and then becomes less rigid. The elongation at break (EB) was found to be decreased to 50.3% (Pure PVA film), 12.77%, 9.39%, 6.14%, and 5.15% with the addition of 5–20 wt. % of CPSP in PVA matrix. The trend observed in elongation at break in the study was similar to the loading of LASP [35] and Green banana peel powder [36] with PVA described in previous studies. The mechanical properties and thickness of film samples are listed in Table 4. The type of fillers and polymer matrices, the concentration of fillers, the interfacial region, and the shape of the fillers can all impact the mechanical properties of polymers [37].

Table 4
Mechanical properties and thickness of film samples

Film Samples	Thickness of films in mm	Tensile strength in MPa	Young modulus in MPa	% of Elongation at break
Pure PVA	0.143	13.72	21.34	50.3
PVA/5wt.% CPSP	0.153	19.84	35.58	12.77
PVA/10wt.% CPSP	0.158	24.95	48.5	9.39
PVA/15wt.% CPSP	0.162	28.81	63.22	6.14
PVA/20wt.% CPSP	0.167	29.93	65.43	5.15
PVA/25wt.% CPSP	0.171	26.95	61.08	6.32

UV-light barrier properties

Effects of various concentrations of Ceiba Pentandra Shell Powder (CPSP) content on the UV-light barrier property of PVA films are shown in Fig. 8, and with the addition of CPSP, the transmittance of PVA films notably decreased at 200–800 nm wavelength, for the PVA films that were filled with 25 wt. % of CPSP's film transmittance diminished from 70–35%. Moreover, the incorporation of 5–25 wt. % of CPSP significantly increased the opacity 'O' value. The PVA film with the highest content (25 wt. %) of CPSP displayed the most significant O value, shown in Fig. 9. The results proved that the light barrier capability of PVA films might be significantly increased by adding various amounts of CPSP particulate filler; when more CPSP is loaded, the PVA film can reveal a more vital light-blocking ability.

The various agro waste particulate fillers were earlier used to improve the light barrier properties of Packaging materials. Film transmittance in the UV and visible ranges decreased in PVA films strengthened with green banana peel powder (Balavairavan et al. 2021). A better film barrier quality was the principal outcome of the stuffing action of agro-waste particle fillers. Another investigation showed that incorporating the alkali-treated LASP (Loganathan et al. 2022) improved the opacity of a biopolymer-based film. The agglomeration of CPSP at higher loading proportions in the PVA matrix was primarily responsible for the decrease in transmittance at 800 nm and the increase in crystallinity generated by increasing the CPSP concentration in the film.

Water absorption test

The limitations of polymeric materials prohibit their widespread usage in numerous applications due to their high-water absorption and solubility [38]. The water absorption properties of various PVA/CPSP film ratios were examined, and Fig. 10, showed the % of water absorption over time. The Fig. 10, shows that adding ceiba pentandra shell powder increases the PVA/CPSP film's water absorption %. This is because the hydrophilic ceiba pentandra shell powder has a high fiber content and is easily influenced by water absorption. The water absorption capacity of the PVA/CPSP films with 5 wt.%, 10 wt.%, 15 wt.%, 20 wt.%, and 25 wt.% of CPSP demonstrated an identical trend, however the percentage of water absorptivity improves with the adding of CPSP content. All of the PVA/CPSP films tend to absorb water after being immersed in water until 5 hours. The film lost their ability to absorb water after 300 minutes because they were saturated with water molecules.

Additionally, the PVA/CPSP films have the lowest % of water absorptivity among all combinations of films despite having the least amount of CPSP (5 wt. %). This is because the ceiba pentandra shell powder is not entirely enclosed by the PVA matrix, which makes the hydroxyl groups of PVA more readily available to water-binding sites. The absorption of water particles inside the films will be impeded by the zigzag path caused by an increase in the amount of CPSP in PVA. As equilibrium conditions were reached, the CPSP particles served as a stiff filler to lock the hydroxyl components interaction, causing the absorption of water by the films to reach saturation [39].

Soil Burial Test

The biodegradability of is a noteworthy property for packaging plastic materials. The seasonal conditions of the soil will provide a realistic environment for film degradation. The degradation occurs under the action of the natural microorganisms (bacteria, fungi, etc.) [40]. Figure 11 showed the indoor soil burial test chamber arrangement.

The effect of ceiba pentandra shell powder on the biodegradability of polyvinyl alcohol films was studied by evaluating the weight loss of the films under the soil burial condition. Figure 12 depicts the weight loss of controlled PVA films and films with various concentrations of CPSP after 2 months of burial time in soil. With an increase in CPSP amount, the weight loss of all combination films changed (increased) significantly, which may imply that CPSP has a considerable impact on the biodegradability of the films. Additionally, tiny voids in films that absorb soil moisture are formed due to the high concentration of CPSP in PVA and reduced film density [41]. As stated in the results of the water intake study, the incorporation of CPSP from 5 wt. % to 25 wt. % increased the hydrophilicity of the films with the hydroxyl groups bonded together. As a result, water absorption of PVA/CPSP films increased, which accelerated the decay of PVA/CPSP films.

According to the prior investigation, weight loss was similarly associated with microbial deterioration of the films. The visually reviewed film samples reflected the weight reduction of all films perfectly (Fig. 8) [42]. In a soil burial test, the control PVA film lost roughly 30.2% of its original weight by the 60th day, but the PVA/5 wt.% of blend film lost 12.51% of its weight in only 20 days. By the 60th day, a significant weight reduction (44.5, 49.3, 52.4, 56.9, and 60.7%) was seen for PVA/CPSP films with 5, 10, 15, 20, and 25 wt. % of CPSP.

Conclusion

Polyvinyl alcohol (PVA) - Ceiba Pentandra Shell Powder (5, 10, 15, 20, and 25 wt. %) biofilms were prepared using the solution casting method, and various tests characterized films. The functional groups of PVA and CPSP interacted well, according to FTIR spectra. The PVA/CPSP biofilms are semi-crystalline, and the crystallinity of biofilms is at 25 wt. % CPSP (48.5%) is comparatively higher than neat PVA (33.2%). Their thermal and mechanical properties influenced the high crystallinity of biofilms. At maximum loading of CPSP (25 wt.%), the minor voids were only visible in the FESEM micrographs, indicating that the particles were evenly distributed and incorporated in the PVA matrix. The PVA/CPSP films were also observed to have increased light absorption against UV radiation. Consequently, the PVA/CPSP biofilms unveiled a substantial enhancement in tensile properties at appropriate loading of CPSP (20 wt. %). The PVA/CPSP films are suitable for applications with temperatures up to 320 ℃. Besides that, water absorption of films increased with increasing the CPSP loading. The fact that both PVA and CPSP are water sensitive and have hydroxyl groups in their chemical structures is considered to be the reason. Based on the soil burial test, the weight losses increased (up to 59% weight loss in 60 days) with increasing CPSP loading, indicating that the films can degrade faster. Polymer films showed a rise in water uptake % with CPSP loading. The ability to absorb the UV-light of PVA/CPSP films also increased.

Declarations

Ethics approval: Not applicable.

Data Availability: Data sharing does not apply to this article as no datasets were generated or analyzed during the current study.

Author's Contributions: M.Kaliraj and P.Narayanasamy conceived the research idea. M.Kaliraj fabricated the various proportions of PVA/CPSP biofilms. B.Balavairavan verified the analytical methods and test results. P.Balasundar investigated the findings of this work. All authors discussed the results and contributed to the final manuscript.

Funding: There is No funding received regarding this research work.

Competing interests: The authors declare that they have no competing interests

References

1. Idumah CI, Obele CM, Ezeani EO (2021) Understanding interfacial dispersions in eco benign polymer nano-bio composites. Polym-Plas Tech and Mater 60(3):233-252. https://doi.org/10.1080/25740881.2020.1811312
2. Skariyachan S, Manjunatha V, Sultana S, Jois C, Bai V, Vasist KS (2016) Novel bacterial consortia isolated from plastic garbage processing areas demonstrated enhanced degradation for low density polyethylene. Envi Sci and Pollut Research 23:18307-18319. https://doi.org/10.1007/s11356-016-7000-y
3. Aattache A (2022) Properties and durability of partially replaced cement-based composite mortars co-using powders of a nano silica super plasticiser and finely ground plastic waste. J Build Engg 51: 104257. https://doi.org/10.1016/j.jobe.2022.104257
4. Asyraf MRM, Ishak MR, Sapuan SM, YidrisN, Ilyas RA, Rafidah M, Razman MR (2020) Potential application of green composites for cross arm component in transmission tower: A brief review. Inter J Polym Sci 1-15. https://doi.org/10.1155/2020/8878300
5. Neto J, Queiroz H, Aguiar R, Lima R, Cavalcanti D, Banea MD (2022) A review of recent advances in hybrid natural fiber reinforced polymer composites. J Renew Mater 10(3): 561. https://DOI:10.32604/jrm.2022.017434
6. PanY, Farmahini-Farahani M, O'Hearn P, Xiao H, Ocampo H (2016) An overview of bio-based polymers for packaging materials. J Bioresour Bioprod 1(3):106-113.
7. Muneer F, Rasul I, Azeem F, Siddique MH, Zubair M, Nadeem H (2020) Microbial polyhydroxyalkanoates (PHAs): efficient replacement of synthetic polymers. J Polym Environ 28: 2301-2323. https://doi.org/10.1007/s10924-020-01772-1
8. Thong CC, Teo DCL, Ng CK (2016) Application of polyvinyl alcohol (PVA) in cement-based composite materials: A review of its engineering properties and microstructure behavior. Construt Build Mater 107:172-180. https://doi.org/10.1016/j.conbuildmat.2015.12.188
9. Mok CF, Ching YC, Muhamad F, Abu Osman NA, Hai ND, Che Hassan CR (2020) Adsorption of dyes using poly (vinyl alcohol)(PVA) and PVA-based polymer composite adsorbents: a review. J Polym Environ 28 :775-793. https://doi.org/10.1007/s10924-020-01656-4
10. Sirivechphongkul K, Chiarasumran N, Saisriyoot M, Thanapimmetha A, Srinophakun P, Iamsaard K, LinYT (2022) Agri-Biodegradable Mulch Films Derived from Lignin in Empty Fruit Bunches. Catalysts 12(10):1150. https://doi.org/10.3390/catal12101150
11. Banerjee M, Jain A, Mukherjee GS (2019) Microstructural and optical properties of polyvinyl alcohol/manganese chloride composite film. Polym Compo 40(S1):E765-E775. https://doi.org/10.1002/pc.25017
12. Gautam S, Sharma B, Jain P (2021) Green Natural Protein Isolate based composites and nanocomposites: A review. Polym Testing 99:106626. https://doi.org/10.1016/j.polymertesting.2020.106626

13. Sapuan SM, Harussani MM , Ismail AH, Zularifin Soh NS, Mohamad Azwardi MI, Siddiqui VU (2023). Development of nanocellulose fiber reinforced starch biopolymer composites: a review. Physi Sci Reviews 0. https://doi.org/10.1515/psr-2022-0007
14. Baraniak J, Kania-Dobrowolska M (2023) Multi-Purpose Utilization of Kapok Fiber and Properties of Ceiba Pentandra Tree in Various Branches of Industry. J Nat Fibers 20(1):2192542. https://doi.org/10.1080/15440478.2023.2192542
15. Patwardhan SB, Pandit S, Ghosh D, Dhar DW, Banerjee S, Joshi S, Kumar Kesari K (2022) A concise review on the cultivation of microalgal biofilms for biofuel feedstock production. Biomass Conver Bio refine 1-18. https://doi.org/10.1007/s13399-022-02783-9
16. Silitonga AS, Mahliaa TM, Ong HM (2012) Ceiba Pentandra: A feasible non-edible oil source for biodiesel production. Seeds 17(24): 28-29.
17. Agustiani V, Khoiriyah L, Matin HHA, Rachmawati S (2022) Effect of hydrogen peroxide acetic acid pretreatment on kapok (ceiba pentandra) fruit peel waste for bioethanol production using separated hydrolysis and fermentation methods. Mater Today Proceedings 63: S73-S77. https://doi.org/10.1016/j.matpr.2022.01.293
18. Daneshfozoun S, Abdullah MA, Abdullah B (2017) Preparation and characterization of magnetic biosorbent based on oil palm empty fruit bunch fibers, cellulose and Ceiba pentandra for heavy metal ions removal. Indus. Crops and Prod 105:93-103. https://doi.org/10.1016/j.indcrop.2017.05.011
19. Da Silva CG, Kano FS, dos Santos Rosa D (2019) Thermal stability of the PBAT biofilms with cellulose nanostructures/essential oils for active packaging. J. Ther. Anal. Calorimetry 138(4):2375-2386. https://doi.org/10.1007/s10973-019-08190-z
20. Soeda J, Uemura T, Okamoto T, Mitsui C, Yamagishi M, Takeya J (2013) Inch-size solution-processed single-crystalline films of high-mobility organic semiconductors. Appl, phys, express 6(7):076503. DOI 10.7567/APEX.6.076503
21. Sisodia R, Jerry K, Das PP, Gupta P, Gupta S, Chaudhary V (2023) Experimental study on mechanical behaviour of linen/epoxy and linen/hemp/epoxy hybrid polymer composite. Mater Today: Proceed 78:372-377. https://doi.org/10.1016/j.matpr.2022.10.176
22. Pagno CH, Costa TM, de Menezes, EW, Benvenutti EV, Hertz PF, Matte CR., Flores SH (2015) Development of active biofilms of quinoa (Chenopodium quinoa W.) starch containing gold nanoparticles and evaluation of antimicrobial activity. Food Chem 173:755-762. https://doi.org/10.1016/j.foodchem.2014.10.068
23. Arman NSN, Chen RS, Ahmad S (2021) Review of state-of-the-art studies on the water absorption capacity of agricultural fiber-reinforced polymer composites for sustainable construction. Construct Build Mater 302:124174. https://doi.org/10.1016/j.conbuildmat.2021.124174
24. Balavairavan B, Saravanakumar SS, Manikandan KM (2021) Physicochemical and structural properties of green biofilms from poly (vinyl alcohol)/nano coconut shell filler. J Nat Fibers 18(12):2112-2126. https://doi.org/10.1016/j.conbuildmat.2021.124174

25. Chhatariya HF, Srinivasan S, Choudhary PM, Begum SS (2022) Corn starch biofilm reinforced with orange peel powder: characterization of physicochemical and mechanical properties. Mater Today: Proceed 59:884-892. https://doi.org/10.1016/j.matpr.2022.01.339

26. BAziz S, S Marf A , Dannoun EM, Brza MA, Abdullah RM (2020) The study of the degree of crystallinity, electrical equivalent circuit, and dielectric properties of polyvinyl alcohol (PVA)-based biopolymer electrolytes. Polymers 12(10): 2184. https://doi.org/10.3390/polym12102184

27. MoriT, MoriT, Fujii A, Saito A, Saomoto, H, Kamada K (2020) Effect of Crystallinity in Stretched PVA Films on Triplet–Triplet Annihilation Photon Up conversion. ACS Appl. Polym. Mater 2(4):1422-1428. https://doi.org/10.1021/acsapm.0c00020

28. Parvej MS, Wang X, Fehrenbach J, Ulven CA (2020) Atomic force microscopy-based nanomechanical characterization of kenaf fiber. J Compo Mater 54(15):2065-2071. https://doi.org/10.1177/00219983198920

29. Yaradoddi JS, Banapurmath NR, Ganachari SV, Soudagar MEM, Mubarak NM, Hallad S, Fayaz H (2020) Biodegradable carboxymethyl cellulose based material for sustainable packaging application. Scien reports 10(1):1-13. https://doi.org 10.1038/s41598-020-78912-z

30. Gisan KA, Chan MY, Koay SC (2022) Solvent-cast biofilm from poly (lactic) acid and durian husk fiber: tensile, water absorption, and biodegradation behaviours. J Nat Fibers 19(11): 4338-4349. https://doi.org/10.1080/15440478.2020.1857894

31. Guimaraes M, Botaro VR, Novack KM, Teixeira FG, Tonoli GHD (2015) High moisture strength of cassava starch/polyvinyl alcohol-compatible blends for the packaging and agricultural sectors. J Polym Research 22:1-18. https://doi.org/10.1007/s10965-015-0834-z

32. Rahmadiawan D, Abral H, Railis RM, Iby IC, Mahardika M, Handayani D, Akbar F (2022) The Enhanced Moisture Absorption and Tensile Strength of PVA/Uncaria gambir extract by Boric Acid as a Highly Moisture-Resistant, Anti-UV, and Strong Film for Food Packaging Applications. J Compo Scien 6(11):337. https://doi.org/10.3390/jcs6110337

33. Zhao D, Feng M, Zhang L, He B, Chen X, Sun J (2021) Facile synthesis of self-healing and layered sodium alginate/polyacrylamide hydrogel promoted by dynamic hydrogen bond. Carbohydrate Polym 256:117580. https://doi.org/10.1016/j.carbpol.2020.117580

34. Asadollahi M, Gerashi E, Zohrevand M, Zarei M, Sayedain SS, Alizadeh R, Atari M (2022) Improving mechanical properties and biocompatibility of 3D printed PLA by the addition of PEG and titanium particles, using a novel incorporation method. Bio printing 27:e00228. https://doi.org/10.1016/j.bprint.2022.e00228

35. Loganathan Saravanakumar SS, Murugan R (2022) Investigation of physico-mechanical, thermal, morphological, optical and biodegradation properties of polyvinyl alcohol films reinforced with alkali treated Limonia acidissima shell powder. Polym Compos 43(6): 3544-3559. https://doi.org/10.1002/pc.26636

36. Balavairavan B, Saravanakumar SS (2021) Characterization of eco-friendly poly (vinyl alcohol) and green banana peel filler (GBPF) reinforced bio-films. J Polym Environ 29:2756-2771.

https://doi.org/10.1007/s10924-021-02056-y

37. Putson C, Jaaoh D, Meauma N, Muensit N (2012) Effect of micro-and nano-particle fillers at low percolation threshold on the dielectric and mechanical properties of polyurethane/copper composites. J Inorgan Organo metal Polym Mater 22:1300-1307. https://doi.org/10.1007/s10904-012-9755-z
38. Liu Y, Ahmed S, Sameen DE, Wang Y, Lu R, Dai J, Qin W (2021) A review of cellulose and its derivatives in biopolymer-based for food packaging application. Trends in Food Scien & Technol 112:532-546. https://doi.org/10.1016/j.tifs.2021.04.016
39. Turan D (2021) Water vapor transport properties of polyurethane films for packaging of respiring foods. Food Engi Reviews 13(1):54-65. https://doi.org/10.1007/s12393-019-09205-z
40. Urbanek AK, Rymowicz W, Mirończuk AM (2018) Degradation of plastics and plastic-degrading bacteria in cold marine habitats. Appl. Microbial. Biotechnol 102:7669-7678. https://doi.org/10.1007/s00253-018-9195-y
41. Yadav J, Chauhan P (2022) Recent Advances in Synthesis, Characterization, and Application of Nanotechnology in Wastewater Treatment - A Review. Nanosci & Nanotechnol -Asia 12(3):16-33. https://doi.org/10.2174/2210681212666220405162938
42. Shankar S, Teng X, Li G, Rhim JW (2015) Preparation, characterization, and antimicrobial activity of gelatin/ZnO nano composite films. Food Hydro coll 45:264-271. https://doi.org/10.1016/j.foodhyd.2014.12.001

Figures

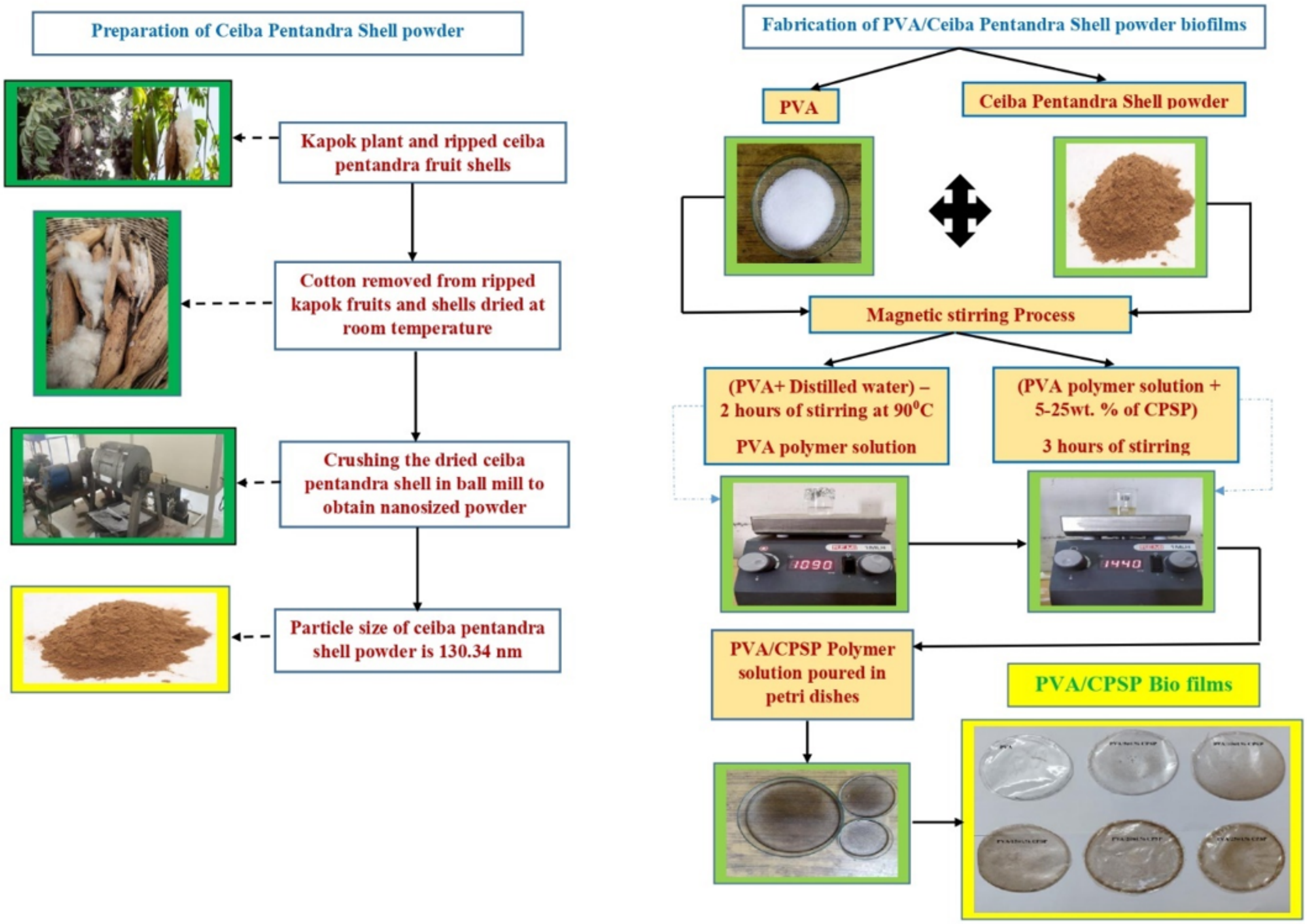

Figure 1

Preparation of Ceiba Pentandra Shell powder and PVA/CPSP biofilms

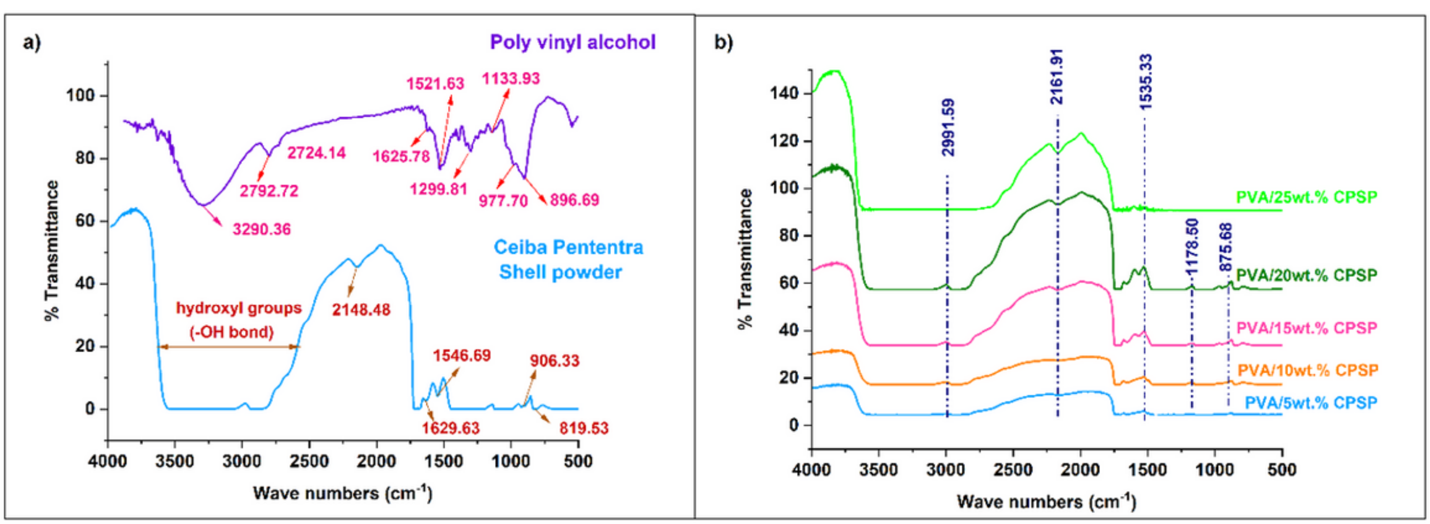

Figure 2

FTIR spectra of (a) Pure PVA and Ceiba Pentandra Shell Powder, (b) PVA/ CPSP (5-25 wt.%) biofilms

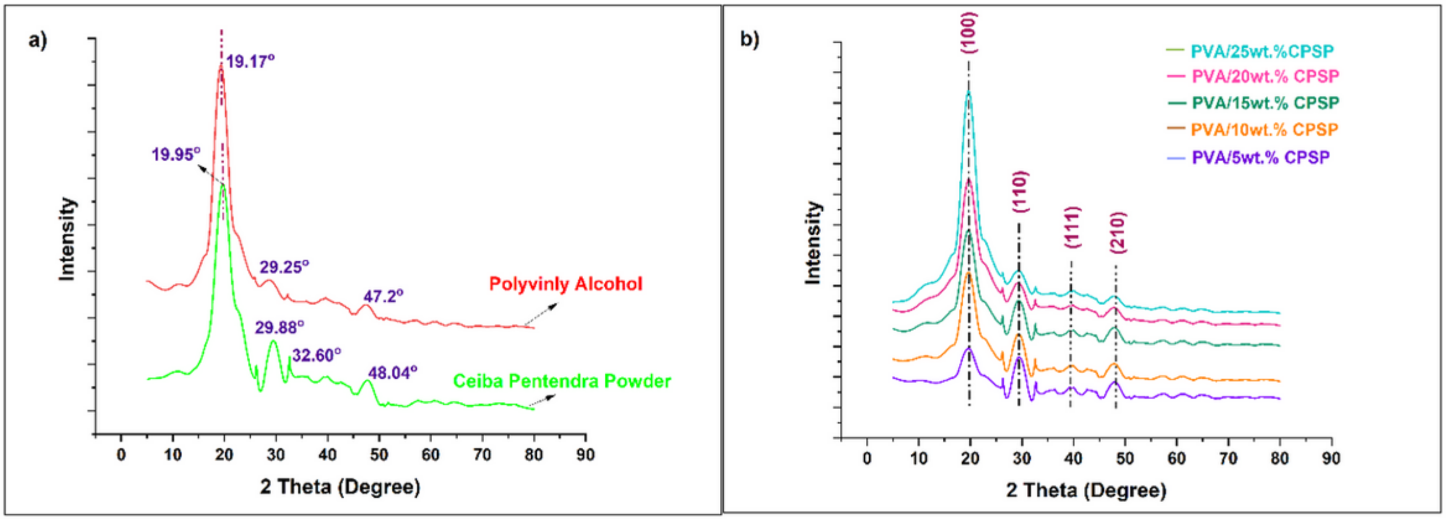

Figure 3

X-Ray diffractograms of (a) Pure PVA and Ceiba Pentandra Shell Powder, (b). PVA/ CPSP (5-25 wt. %) biofilms

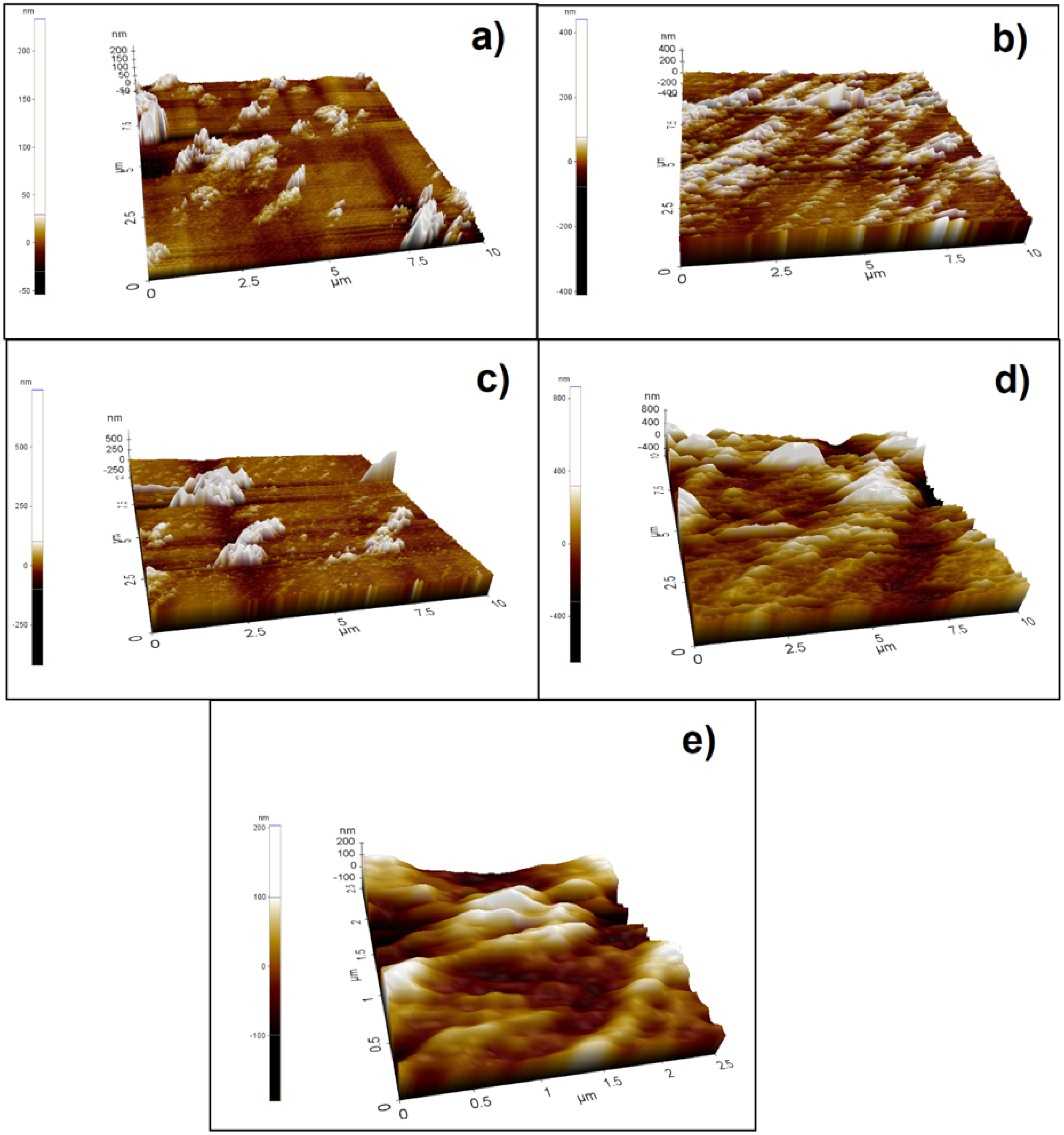

Figure 4

AFM micrographs of (a). PVA/5 wt. % CPSP film, (b). PVA/10 wt. % CPSP film, (c) PVA/15 wt. % CPSP film, (d). PVA/20 wt. % CPSP film, (e). PVA/25 wt. % CPSP film

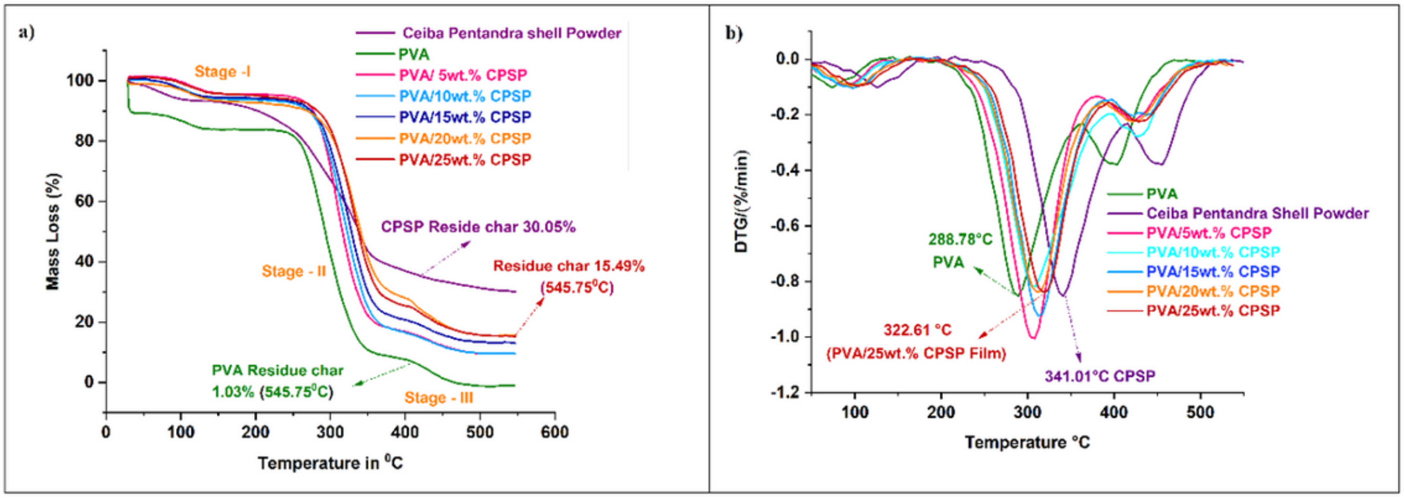

Figure 5

(a) Primary thermograms of PVA, CPSP & PVA/CPSP biofilms, (b) Secondary thermograms of PVA, CPSP & PVA/CPSP biofilms

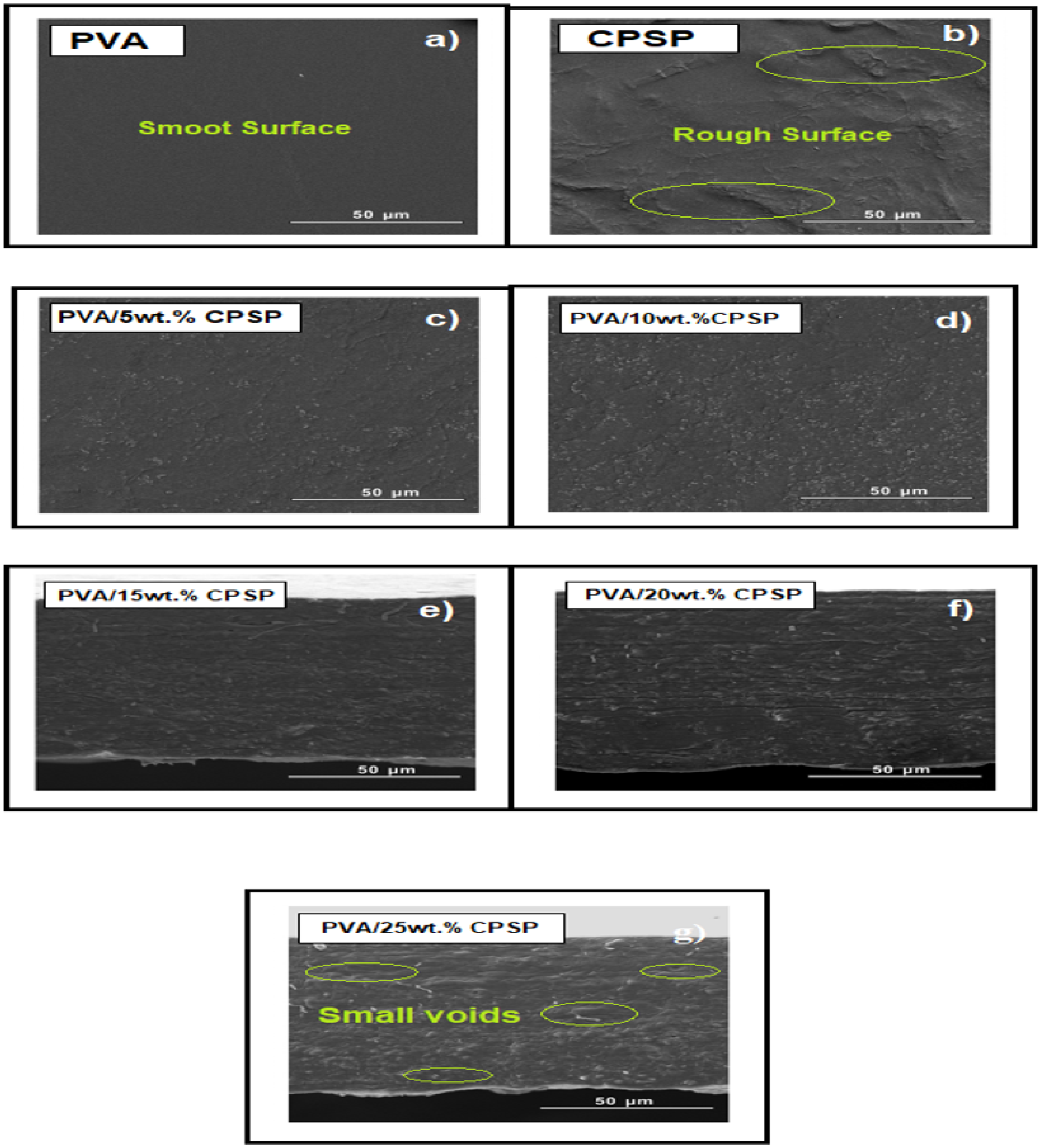

Figure 6

FESEM images of PVA, CPSP, and PVA/ CPSP (5-25 wt.%) biofilm samples

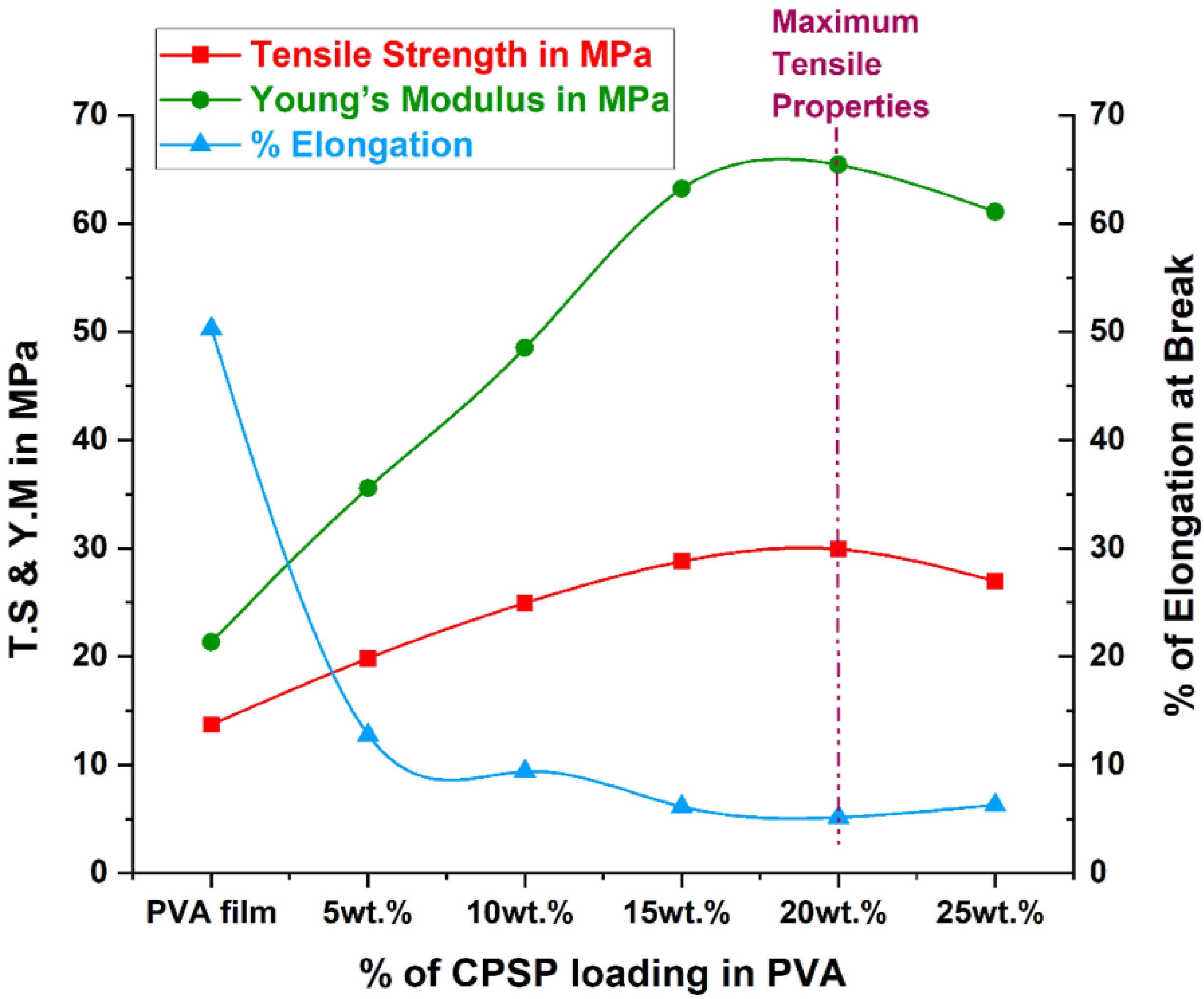

Figure 7

Tensile properties of PVA and PVA/CPSP (5-25wt.%) biofilms

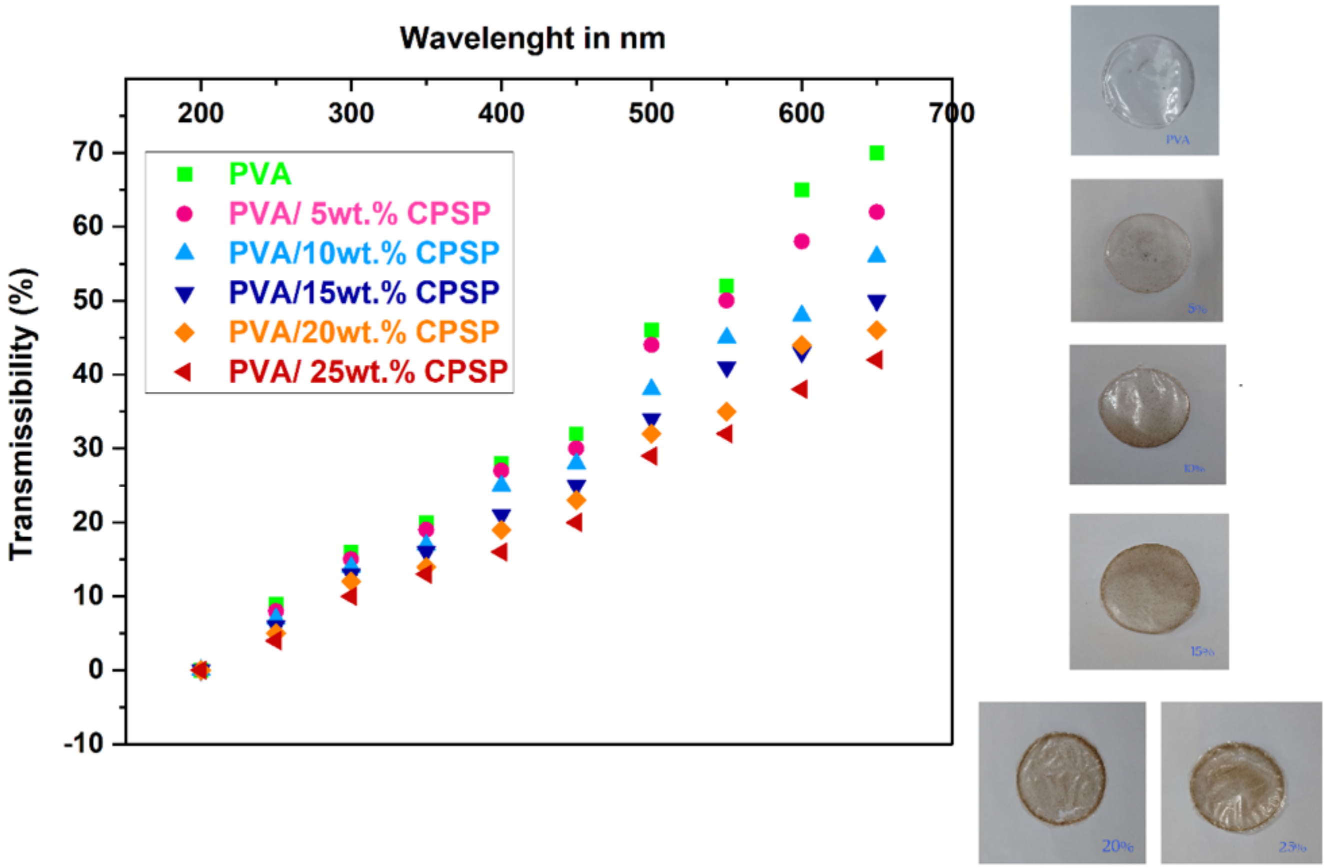

Figure 8

Transmissibility of Pure PVA and PVA/ (5-25 wt.% CPSP) biofilms

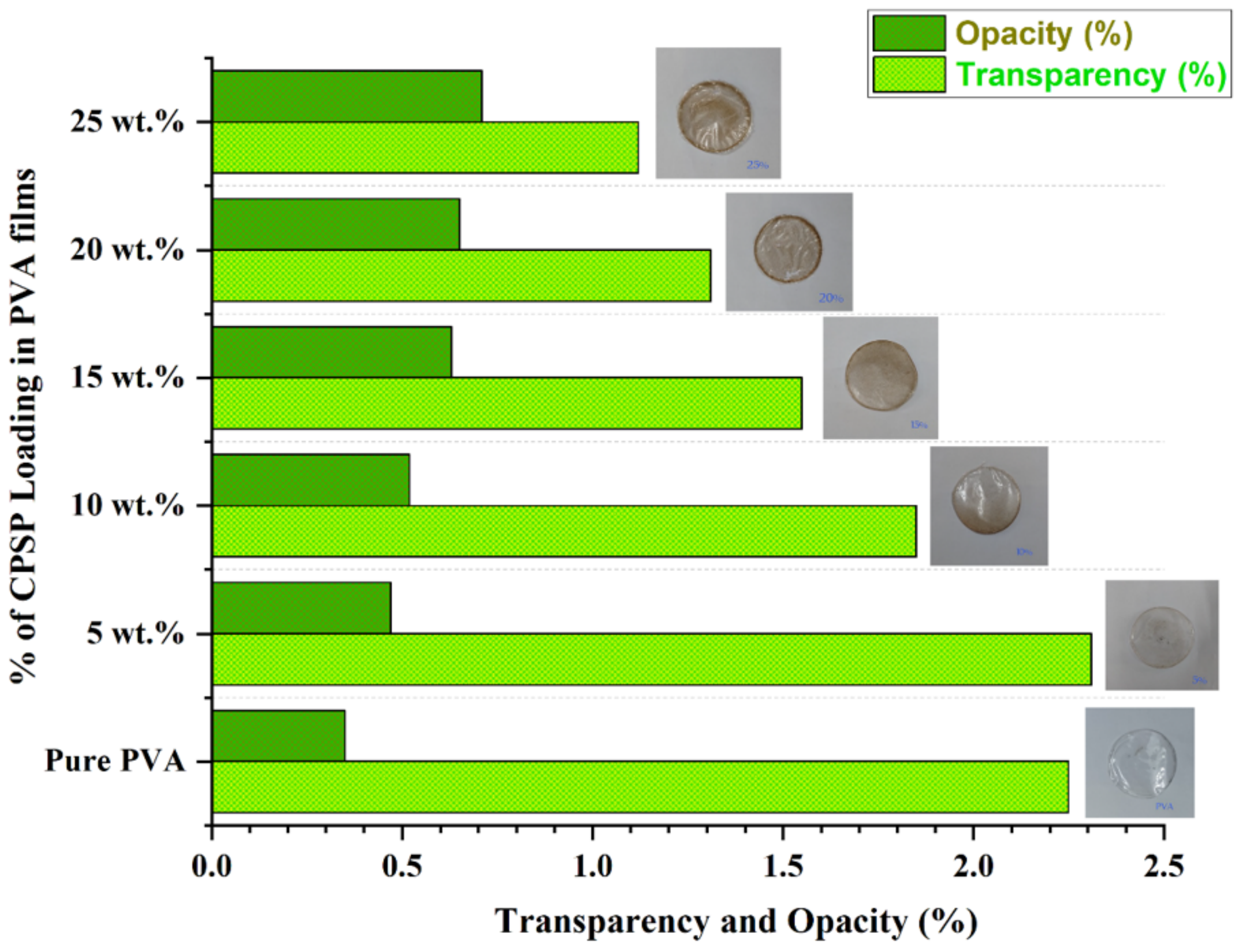

Figure 9

Opacity of Pure PVA and PVA/CPSP biofilms

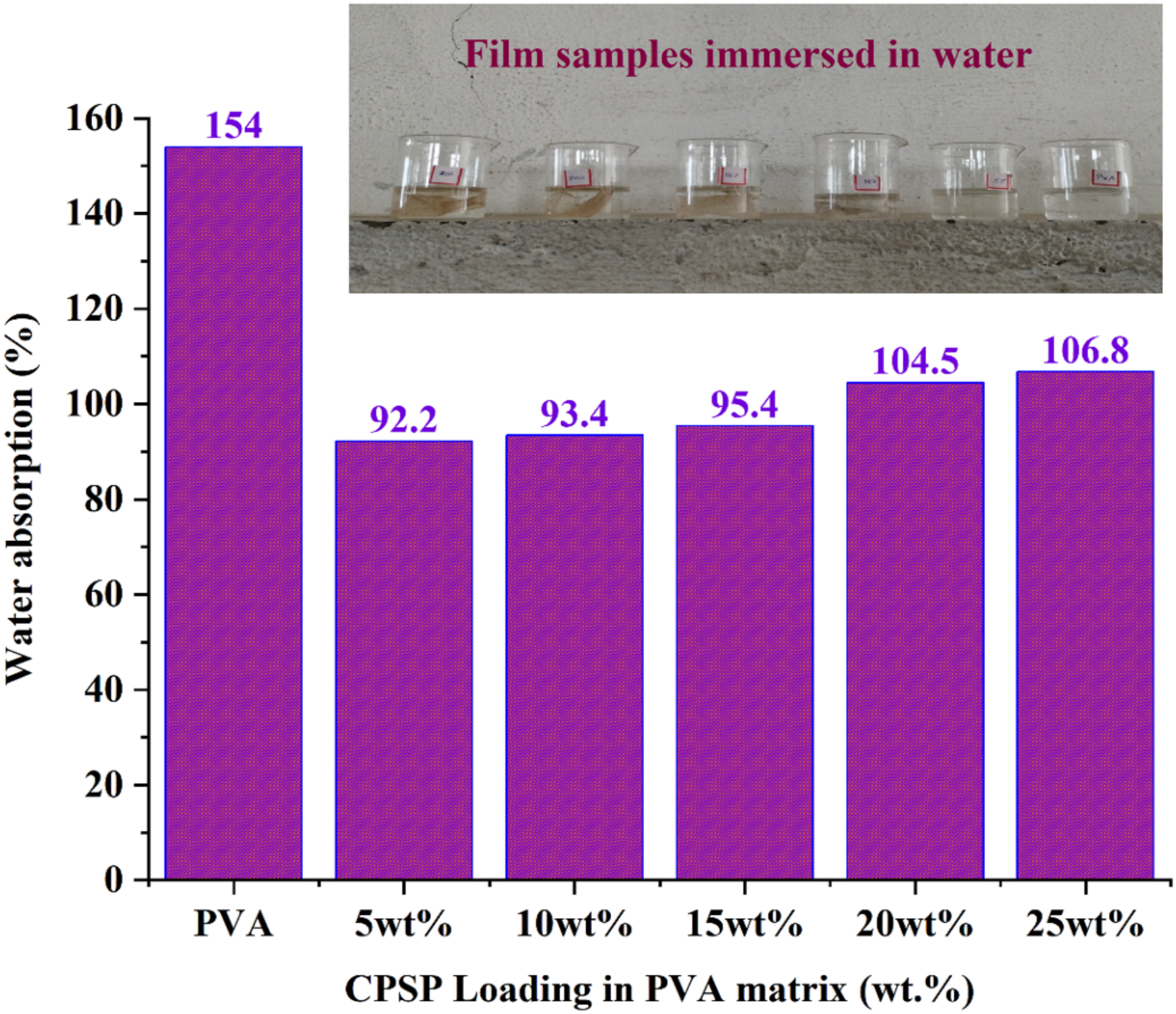

Figure 10

% Water absorption of PVA and PVA/CPSP biofilms

Figure 11

Indoor soil burial test set up

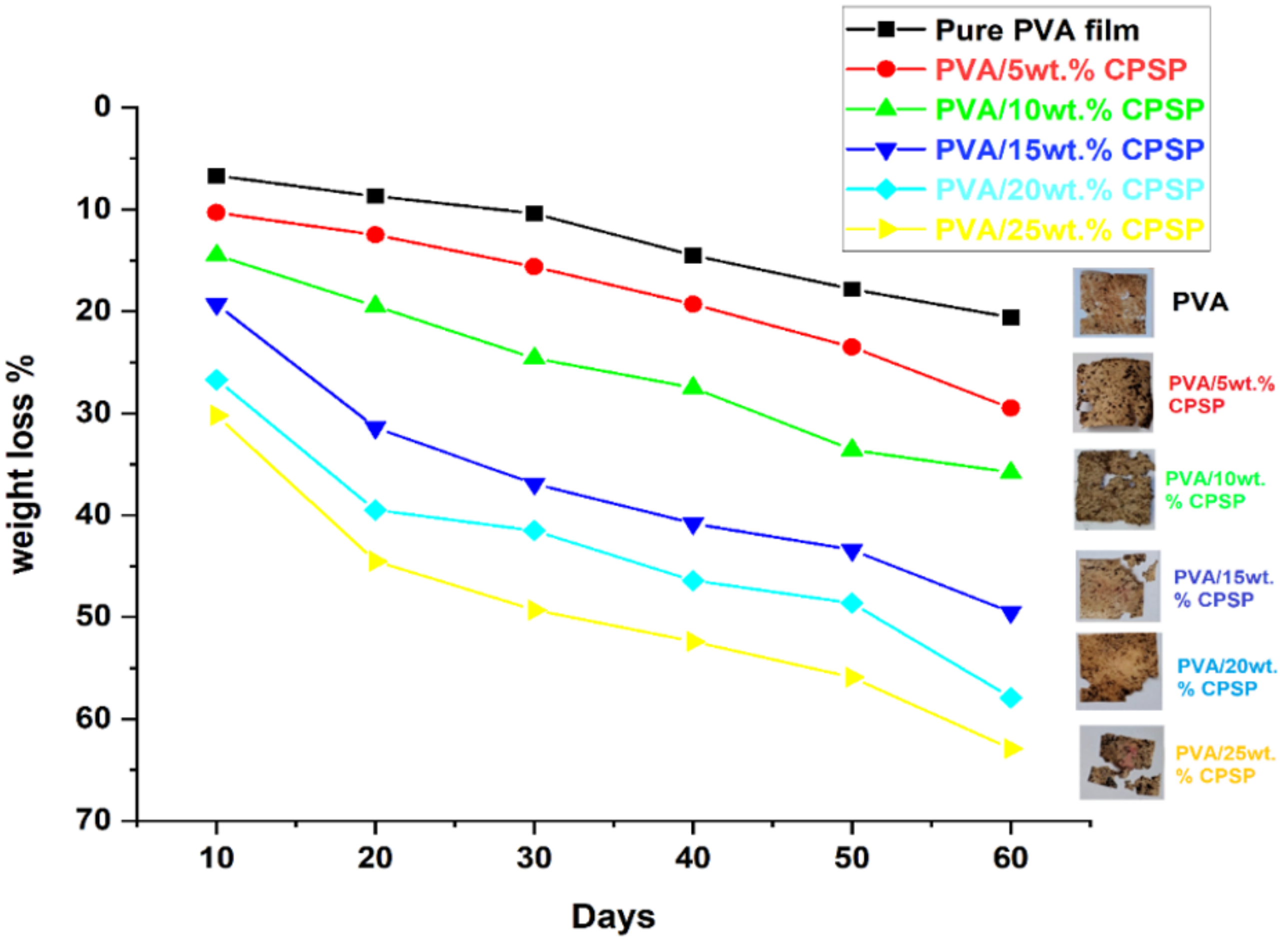

Figure 12

% weightloss of PVA and PVA/CPSP (5-25wt.%) biofilms